SOCAR Proceedings

Geology, Geophysics & Formation Evaluation

journal home page: http://proceedings.socar.az

GEOCHEMICAL AND MINERALOGICAL CHARACTERISTICS OF UPPER CRETACEOUS SEDIMENTS IN THE LOK-KARABAKH ZONE (AZERBAIJAN): IMPLICATIONS FOR PROVENANCE, PALEOWEATHERING, PALEOCLIMATE AND RESERVOIR PREDICTION

E. G. Aliyeva, E. Kh. Guliyev*

Ministry of Science and Education of the Republic of Azerbaijan,
Institute of Geology and Geophysics, Baku, Azerbaijan

A B S T R A C T

This study investigates the tectonic setting, sediment provenance, paleoweathering, paleoclimate, and hydrothermal influences on the Upper Cretaceous deposits of the Lok-Karabakh Zone using geochemical and mineralogical data. The results indicate that the sediments were primarily derived from volcanic arc-related mafic to intermediate rocks and deposited in an arc-related basin. Major and trace element analysis suggests that the sediments originated predominantly from volcaniclastic and terrigenous sources. The Chemical Index of Alteration (CIA) values range from 52 to 95, indicating a low to moderate degree of weathering, with most samples reflecting a cold and arid climate. Mineralogical data further support moderate chemical weathering, with montmorillonite as the dominant clay mineral, along with kaolinite, chlorite, and illite. The A-CN-K ternary diagram suggests plagioclase weathering as the dominant alteration pathway, with limited potassium enrichment. Elemental discrimination diagrams confirm a minimal hydrothermal influence, as evidenced by the Al–Fe–Mn ternary diagram and metalliferous index values exceeding 0.4. Tectonic discrimination diagrams reveal that the sediments were deposited in an arc-related basin influenced by subduction-driven processes. The geochemical proxies indicate that the Lok-Karabakh sedimentary basin was characterized by a scarcity of coarse-grained sediments, leading to a predominance of fine-grained, feldspar-rich deposits such as greywackes, which adversely affected reservoir properties. These findings contribute to a better understanding of the geodynamic evolution of the Lok-Karabakh zone during the Late Cretaceous, highlighting the interplay of arc volcanism, climate, and weathering processes in shaping the sedimentary record. Additionally, the results provide insights into sedimentary basin evolution and reservoir potential in similar geological settings.

Keywords: Upper Cretaceous, Lok-Karabakh zone; paleoweathering; hydrothermal influence; provenance; tectonic setting.

Date submitted: 11.10.2024 **Date accepted:** 14.02.2025

© 2025 «OilGasScientificResearchProject» Institute. All rights reserved.

1. Introduction

The geochemical composition of clastic sedimentary rocks is influenced by source rock provenance, weathering intensity, transportation, depositional environments, and post-depositional processes. These factors shape the mineralogical and chemical characteristics of sediments, providing insights into tectonic settings, basin evolution, and paleoclimate. Chemical weathering, closely linked to paleoclimatic conditions, leads to the alteration of unstable minerals, with varying intensity under different climatic regimes. Additionally, the tectonic setting plays a key role in controlling provenance and hydrothermal activity, where subduction zones, island arcs, and rift systems often exhibit hydrothermal alterations, modifying geochemical signatures. Elemental enrichments, particularly in Fe, Mn, and Ti, may indicate hydrothermal influence. [1, 2]. Despite the significance of these processes, the geochemical evolution of Upper Cretaceous deposits in the Lok-Karabakh Zone remains poorly studied. This study aims to reconstruct the tectonic setting, sediment provenance, paleoweathering, and paleoclimate of the region during the Late Cretaceous, while also evaluating hydrothermal influences on sediment composition.

2. Geological setting

The Lok-Karabakh Zone is a structural unit within the Artvin-Karabakh Uplift, forming part of the South Caucasian microplate and evolving under an island arc geodynamic regime during the Alpine tectonic stage. Within the Lok-Karabakh Zone, the northern downthrown flank forms the Gazakh-Agburun synclinal belt (subzone). The Jurassic core of the fold zone consists of several subzones: in the west and northwest, the Shamkir subzone, which includes the Shamkir and Goygol uplifts, and the Murovdag

**E-mail:* guliyevemin@outlook.com
http://dx.doi.org/10.5510/OGP20250101036

anticline subzone, separated by the Galakend-Dashkesan-Kapaz synclinal subzone. To the east and southeast, the Agdam and Karabakh anticline subzones are located, with the Khachinchay-Khojavand synclinal subzone between them (fig.1) [3].

The Upper Cretaceous deposits of the Lok-Karabakh Zone in the Lesser Caucasus are extensively developed, forming a nearly continuous belt along the northeastern foreland, encompassing the Shamkir and Murovdag anticlinoria and significantly expanding within the Gazakh, Agjakend, and Khojavend synclinal zones.The Cenomanian deposits in the northern foothills of the Lesser Caucasus are widely distributed and primarily composed of sandstones with tuffogenic material, tuffites, and pelitomorphic limestones, interbedded with various clay layers, as observed in the Tezekend section. In the Gazakh syncline and the western part of the Agjakend depression, the Upper Coniacian and Lower Santonian deposits form a volcanogenic-sedimentary sequence, consisting of porphyritic rocks, their tuffs, tuff breccias, and conglomerates, interbedded with sandstones, argillites, limestones, and, more rarely, dark-gray laminated clays, with a thickness ranging from 400 to 1200 meters. The Maastrichtian deposits within the Lok-Agdam Zone exhibit a more limited distribution compared to the Santonian and Campanian formations [4].

3. Methodology

Samples were collected from four outcrops on the northeastern slope of the Lesser Caucasus: Tezekend (Shamkir), Agdam (Tovuz), Hadjikend (Ganja), and Ashygly (Goygol) (fig. 1.). The studied rocks primarily include clayey sandstones, mudstones, and volcanogenic-sedimentary rocks. Quantitative analysis of major elements, trace elements, and rare earth elements (REEs) was conducted using inductively coupled plasma mass spectrometry (ICP-MS) at the Geochemistry, Geochronology, and Isotope Geology Laboratory, Department of Earth Sciences, University of Milan Statale, Italy. The mineralogical composition of the rocks was analyzed using the MiniFlex 600 X-ray diffractometer at the Institute of Geology and Geophysics, Ministry of Science and Education of Azerbaijan.

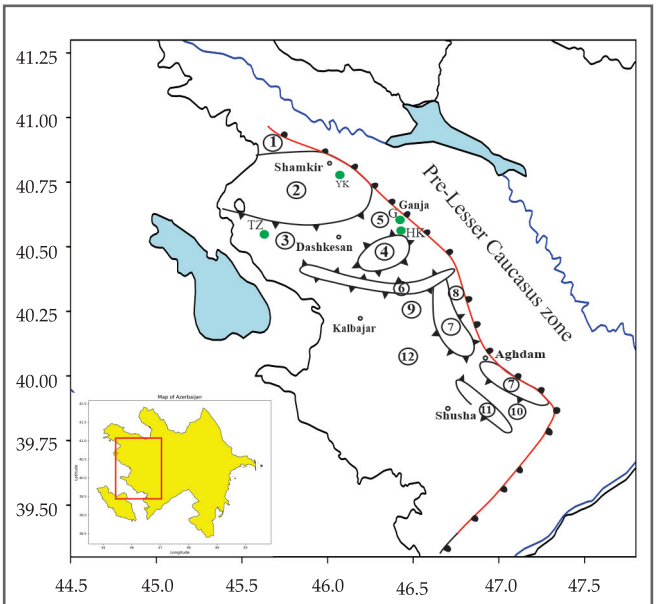

Fig. 1. Major structural elements of the northeastern foreland of the Lesser Caucasus

4. Mineralogy

The analysed rocks exhibit a complex mineralogical composition, including silicates (quartz, feldspar), carbonates (calcite), oxides (hematite), and clay minerals (montmorillonite, kaolinite, chlorite, and illite). Additionally, volcanic ash, composed of both amorphous and crystalline components, was identified. Among the clay minerals, montmorillonite (21.4%) is the most abundant, whereas in certain samples, chlorite (15.7%) exceeds the proportions of illite (5%) and kaolinite (8.17%), indicating variability in mineral composition across the studied rocks.

5. Geochemistry

The major and trace element composition of the analyzed rocks from the Lok-Karabakh Zone (table 1 and 2) follows a distinct geochemical trend within the Upper Cretaceous deposits. The oxide distribution exhibits a systematic decrease in concentration: $SiO_2 > Al_2O_3 > Fe_2O_3 > CaO > MgO > K_2O > Na_2O > TiO_2 > P_2O_5 > MnO$, highlighting the dominance of silica and alumina, with progressively lower proportions of other major oxides. The enrichment of Fe_2O_3 and TiO_2 suggests the presence of iron- and titanium-bearing heavy minerals, likely influencing the sediment's provenance. The increase in CaO, accompanied by a rise in MgO in certain samples, indicates the presence of dolomite; however, the enrichment in MgO is primarily attributed to the presence of chlorite. Trace element analysis reveals a depletion relative to Post-Archean Australian Shale (PAAS) [5], except for Sc, V, and Co. Additionally, samples from the Hadjikend section exhibit notable Ni enrichment (200–351 ppm).

6. Hydrothermal influence

Hydrothermal components and their quantitative contributions to sediments can be assessed using various elemental discrimination diagrams. Element ratios such as Al/(Al+Fe+Mn) and (Fe+Mn)/Ti have proven to be effective indicators of hydrothermal sedimentation. Low TiO_2 and Al_2O_3 content are the typical characters of the hydrothermal siliceous rocks. The metalliferous index, defined as Al/(Al+Fe+Mn), serves as a useful tool for identifying hydrothermal components in different sediment types. This ratio tends to decrease as the hydrothermal contribution increases. Typically, pelagic deep-sea sediments exhibit a metalliferous index greater than 0.4, whereas metal-enriched sediments have values below this threshold [5, 6].

In our study, the samples exhibit significantly elevated ratios of Al/(Al+Fe+Mn) (values exceeding 0.4), which are comparable to those observed in MORB and volcaniclastic particles (VCP) (fig. 2a). The Al–Fe–Mn ternary diagram further substantiates this interpretation by distinctly separating sediments enriched in volcanic and terrigenous material from those with hydrothermal signatures, confirming the predominance of non-hydrothermal components in the samples (fig. 2b) [8, 9].

Table 1

Major element content in representative samples of the Lok-Karabakh zone

Nº Sample	Geological age	SiO_2	TiO_2	Al_2O_3	Fe_2O_3	MnO	MgO	CaO	Na_2O	K_2O	P_2O_5
PK-7	Cenomanian	54.57	0.97	17.93	13.61	0.45	3.22	1.38	0.56	1.06	0.17
PK-10		55.87	0.77	19.34	8.29	0.10	4.01	0.62	0.61	2.25	0.14
PK-11		50.11	0.80	19.87	15.47	0.11	3.14	0.90	0.89	2.40	0.21
PK-12		52.83	0.90	16.41	10.76	0.17	3.25	5.25	2.88	0.72	0.22
PK-16		57.88	0.68	15.41	9.13	0.27	4.90	0.64	0.15	1.35	0.11
TZ-3		60.05	0.70	16.56	6.04	0.19	2.28	2.43	6.33	1.52	0.25
HK-2	Coniacian	47.94	0.84	10.23	7.42	0.15	6.32	8.49	0.93	1.93	0.16
HK-3		48.98	0.82	10.61	8.30	0.11	6.52	6.85	0.90	1.94	0.15
HK-4		46.41	0.83	10.39	8.19	0.10	7.34	8.03	0.94	2.02	0.15
HK-8		57.63	0.98	9.39	11.55	0.09	5.01	4.78	0.62	2.29	0.16
HK-9		60.20	0.75	9.55	7.27	0.07	4.93	4.01	0.82	1.82	0.14
G-10	Lower Santonian	54.58	1.10	14.49	11.16	0.11	2.79	3.99	1.01	3.18	0.25
G-11		56.57	1.09	16.10	11.28	0.08	2.84	1.64	1.04	2.65	0.14
G-12		58.45	1.12	16.34	9.69	0.12	2.73	2.57	1.11	3.31	0.12
PAAS*		62.8	1.0	18.9	6.5	0.11	2.2	1.3	1.2	3.7	0.16

** Taylor and McLennan (1985) [5]*
PAAS (Post-Archean Australian Shale)

Table 2

Content of trace elements in representative samples of the Lok-Karabakh Zone

Nº Sample	Trace elements (ppm)															
	Sc	V	Co	Ni	Ga	Rb	Sr	Y	Zr	Nb	Cs	Ba	Hf	Ta	Th	U
PK-10	29.87	220.47	11.67	2.69	17.81	73.97	135.02	18.55	54.4	2.2	2.08	326.42	1.61	0.11	0.82	3.47
PK-11	27.68	227.1	13.17	4.62	16.68	72.1	140.19	16.75	49.57	2.04	2.16	303.84	1.52	0.13	0.89	3.2
PK-12	26.81	231.27	12.68	3.82	16.97	70.1	475.6	33.21	78.15	2.65	3.35	72.06	2.3	0.13	1.97	1.72
PK-16	27.68	270.03	23.57	12.93	15.78	41.64	47.57	13.43	33.29	1.5	1.85	258.26	1.01	0.08	0.6	3.53
TZ-3	14.27	103.75	12.24	1.15	16.38	29.7	233.16	20.82	122.3	12.12	2.9	219.57	2.95	0.72	2.2	0.73
HK-2	20.22	155.68	43.01	328.23	13.61	64.36	194.86	21.62	133.31	13.77	3.08	127.47	3.39	0.83	4.35	1.07
HK-3	22.36	159.17	46.61	326.56	15.06	69.64	151.18	20.53	120.89	11.51	3.33	118.11	3.07	0.69	3.64	1.11
HK-4	21.89	160.22	28.34	351.62	13.56	68.67	165.72	21.18	123.29	12.79	3.24	135.59	3.06	0.76	3.57	0.95
HK-8	20.69	154.62	32.71	264.68	12.74	67.89	146.84	18.02	113.65	12.10	3.43	124.49	2.95	0.87	3.51	1.02
HK-9	18.99	151.72	18.82	200.80	11.93	67.11	142.49	15.32	104.76	10.00	3.13	130.88	2.64	0.57	3.38	0.92
PAAS*	16	150	23	55	20	160	200	27	210	19	15	650	5.0	-	14.6	3.1

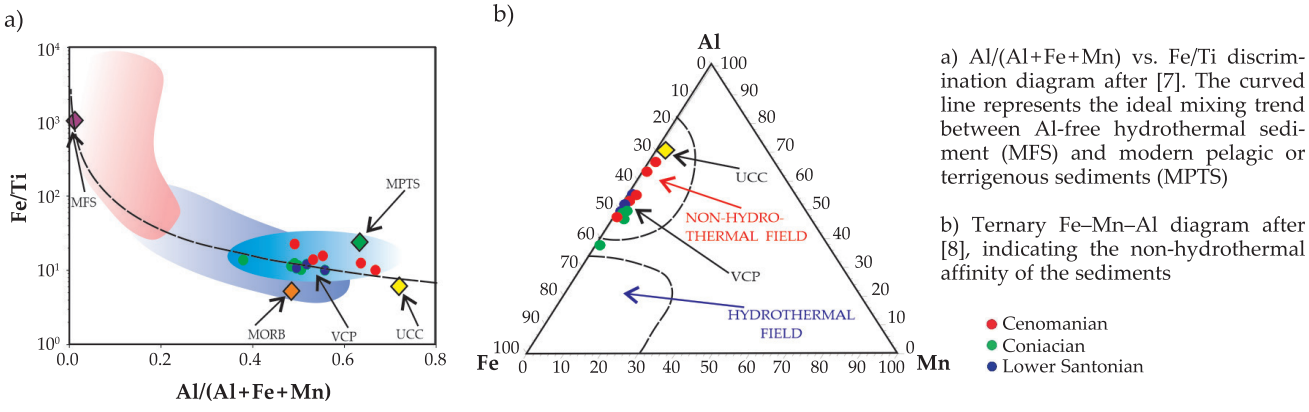

a) Al/(Al+Fe+Mn) vs. Fe/Ti discrimination diagram after [7]. The curved line represents the ideal mixing trend between Al-free hydrothermal sediment (MFS) and modern pelagic or terrigenous sediments (MPTS)

b) Ternary Fe–Mn–Al diagram after [8], indicating the non-hydrothermal affinity of the sediments

Fig. 2. Discrimination diagrams for hydrothermal and non-hydrothermal sediment affinity

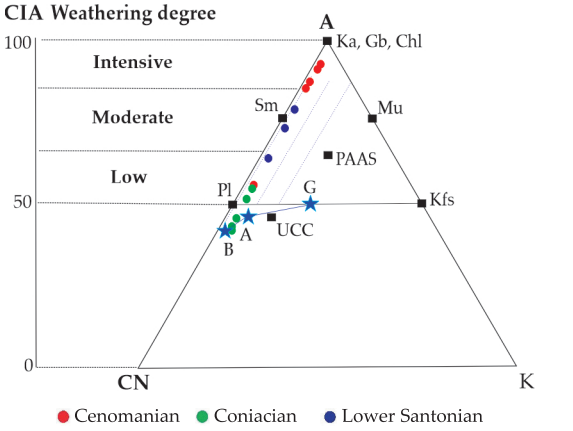

UCC- Upper Continental Crust; PAAS- Post Archean Australian Shale; Ka=kaolinite; Gb=gibbsite; Chl=chlorite; Mu=muscovite; Kfs=K-feldspar; Pl=plagioclase; Sm=smectite
Stars:
A=andesite; B=basalt; G=granite represent typical primary source trend

Fig. 3. Ternary diagram (ACNK) with end members Al_2O_3, $CaO+Na_2O$, and K_2O for starting and residual compositions plotted in mole percent

7. Provenance weathering and paleoclimate

Weathering plays a pivotal role in reshaping the source region's landscape and volume of the sediment supply, thereby influencing the sedimentary basin's overall composition. The amount and grain-size of clastic material coming to depositional basin is directly affected by the scale of weathering. Also, there is a unique example of reservoir rocks formed in the highly weathered magmatic rocks in Muradkhanly field in the Middel Kura basin, Azerbaijan. Thus, understanding of the weathering process is one of the important stages enabling reservoir prediction.

We used in this study to assess the weathering process the chemical index of alteration ($CIA=100\times[Al_2O_3/(Al_2O_3+CaO^*+Na_2O+K_2O)]$, with CaO* representing only the calcium in silicate minerals), which is widely employed in studies of shales and sandstones. Its variations can also indicate past climatic and tectonic influences on weathering intensity. The classifications by Fedo et al. [10] and Nesbitt and Young [11] provide a framework for interpreting weathering intensity and associated climates. Nesbitt and Young [11] suggested that CIA values between 50 and 65 reflect early-stage chemical weathering in cold and arid climates, values between 65 and 85 signify moderate weathering in warm and humid environments, and values between 85 and 100 correspond to intense weathering in hot and humid conditions. However, CIA values must be interpreted cautiously, considering factors such as parent rock composition, diagenesis, and post-depositional alterations. Integrating CIA with other geochemical and mineralogical data enhances the reliability of weathering and climatic reconstructions. The bulk composition of the samples may have been altered due to extensive K-metasomatism and metamorphism, leading to potassium enrichment that requires correction [10, 12]. The corrected K_2O content in weathered samples can be estimated using the approach proposed by [12]: $K_2O_{corr}=m\cdot A+m\cdot(C^*+N)/(1-m)$, where $m=K/(A+C^*+N+K)$ for the protolith sample. In this equation, A represents the molar concentration of Al_2O_3, (C^*+N) corresponds to the sum of CaO* and Na_2O, and K denotes K_2O. The CaO* indicates that calcium oxide has been adjusted to exclude non-silicate contributions. Therefore, applying this correction is essential for obtaining a more accurate representation of the original geochemical composition. By adjusting for K-metasomatism, the modified CIA and other geochemical proxies can more reliably reflect weathering intensity and paleoenvironmental conditions. For the samples in this study, CIA values range from 52 to 95, indicating a broad spectrum of chemical weathering intensities. Most samples, except for those of Cenomanian age, exhibit low to moderate weathering intensity, suggesting exposure to weathering processes under relatively stable climatic conditions. The increase in weathering intensity observed in Cenomanian samples may be linked to tectonic uplift and associated basin shallowing during the Early Cenomanian in the Lesser Caucasus [4].

The A-CN-K (Al_2O_3-CaO^*+Na_2O-K_2O) diagram also helps in assessing the intensity and pathway of weathering by illustrating the depletion of mobile elements and the retention of relatively immobile components such as Al_2O_3. In this ternary A-CN-K diagram [13], the samples plot along the weathering trend for basalt compositions, indicating a chemical alteration pathway dominated by the removal of Ca and Na from plagioclase, with limited potassium enrichment (fig. 3).

The predominance of montmorillonite in the studied rocks also supports the interpretation of moderate weathering intensity, as smectite-group clays typically form under conditions where chemical alteration is neither minimal nor extreme. Montmorillonite develops through the partial breakdown of feldspars and volcanic material, indicating that while weathering was sufficient to alter primary minerals, it did not progress to the formation of more advanced weathering products like kaolinite or gibbsite. This mineralogical composition is closely linked to the cold and dry climatic conditions of the region [14]. In such environments, weathering is primarily driven by periodic, seasonal precipitation, which limits the leaching of major elements (Ca, Na, K) and helps preserve the chemical characteristics of the source rock province. This conclusion is reinforced by the distribution of fine-grained clastic rock compositions on the Ga/Rb–K_2O/Al_2O_3 diagram [15], where the data points fall within the field characteristic of sediments formed under cool and semi-arid and semi-humid climatic conditions (fig. 4).

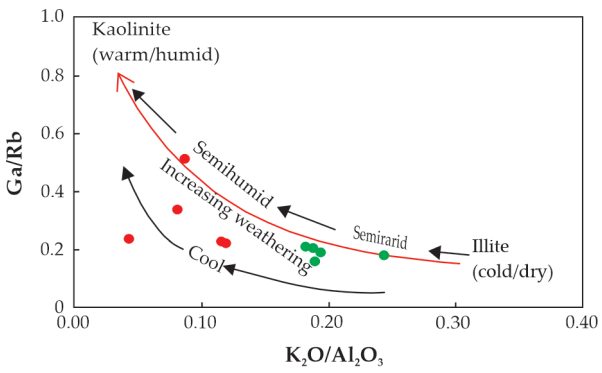

Fig. 4. Ga/Rb-K_2O/Al_2O_3 plot for the clayey sediments

8. Provenance attribute and tectonic setting

The provenance of the source material was determined using the Roser and Korsch (1988) diagram [16], which effectively identifies the sources of sedimentary rocks based on major rock-forming oxides (TiO_2, Al_2O_3, Fe_2O_3, MgO, CaO, Na_2O, K_2O). This diagram distinguishes four types of source rocks: igneous rocks (mafic, intermediate, felsic) and quartz-rich sediments. SiO_2 and CaO were excluded from the calculations due to their mixed terrigenous and authigenic origins, which could introduce variability in the interpretation (fig. 4). The majority of the sample points are clustered within the mafic rock field (P1), with some positioned in the intermediate rock field (P2). Notably, the samples from the Coniacian stage fall within the P1ext field, which is indicative of immature sediments sourced from oceanic island arcs (fig. 5a).

Traditional tectonic discrimination diagrams have faced criticism in recent years due to their limitations in effectively distinguishing between continental island arcs (CIAs) and active continental margins (ACMs), as well as their inability to reliably differentiate among arc, collision, and continental rift settings. Consequently, determining the tectonic setting often necessitates the use of multiple diagrams. To address these limitations, Verma and Armstrong-Altrin (2013) [17] developed a new discriminant function-based diagram capable of distinguishing between continental rift, island arc, and continental collision environments. In the $DF2_{(Arc\text{-}Rift\text{-}Col)m1}$ versus $DF1_{(Arc\text{-}Rift\text{-}Col)m1}$ discrimination diagram (fig. 5b), the majority of the analyzed samples plot within the arc field, suggesting that they were deposited in an arc-related basin influenced by volcanic arc processes.

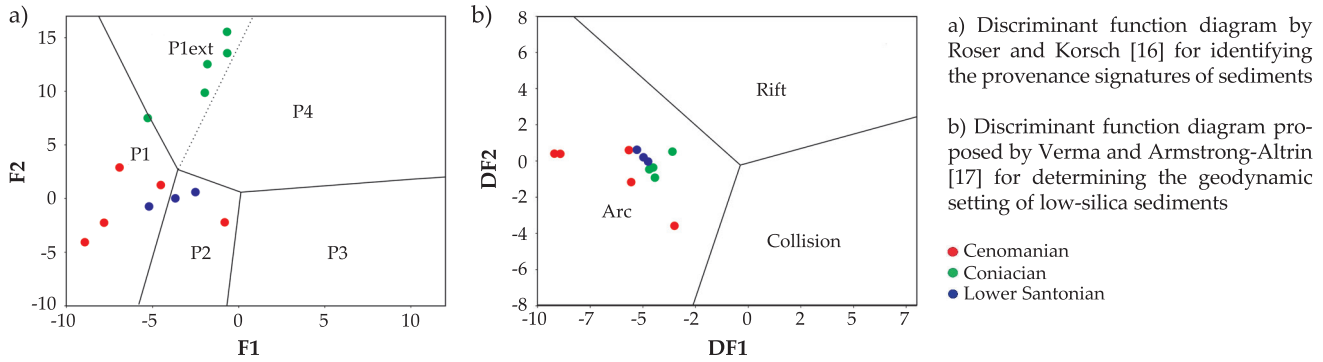

a) Discriminant function diagram by Roser and Korsch [16] for identifying the provenance signatures of sediments

b) Discriminant function diagram proposed by Verma and Armstrong-Altrin [17] for determining the geodynamic setting of low-silica sediments

Fig. 5. Provenance and geodynamic setting discrimination diagrams for sedimentary deposits

Conclusions

1. Geochemical and mineralogical analyses confirm that the Upper Cretaceous sediments of the Lok-Karabakh Zone were derived from mafic to intermediate volcanic-related rocks. Tectonic discrimination diagrams indicate deposition in a basin influenced by subduction-driven processes.
2. The Chemical Index of Alteration (CIA) values predominantly indicate low to moderate weathering intensity across most samples. Notably, Cenomanian samples exhibit higher degrees of weathering, likely attributable to tectonic uplift during that period. The predominance of montmorillonite supports moderate chemical weathering under a cool, semi-arid to semi-humid climate, as confirmed by the $Ga/Rb–K_2O/Al_2O_3$ diagram.
3. Elemental discrimination diagrams and the Al–Fe–Mn ternary plot confirm a minimal hydrothermal contribution. The metalliferous index values exceeding 0.4 indicate that the sediments were mainly sourced from volcaniclastic and terrigenous material rather than hydrothermal processes.
4. The cold-arid climate during investigated time-period predetermined the low - medium degrees of weathering allowing us to assume that Cretaceous Lok-Garabakh sedimentary basin was, probably, coarse sediment starved basin. It is affected the depositional process and accumulation of possible reservoir rocks as well as the reservoir properties of clastic rocks here. Also, the dominating mafic rocks in the provenance area suppose accumulation of feldspar - rich terrigenous material in the depositional basin, including greywackes. All mentioned reduced reservoir properties of the Cretaceous sediments and allow to predict in Lok-Garabakh zone the limited occurrence of coarse clastics displaying low-medium reservoir properties.

References

1. Bilobé, J. A., Takem Eyong, J., Samankassou, E. (2022). Provenance, paleoweathering, depositional setting and paleoclimatic constraints of Cretaceous and Neogene deposits of the Mamfe Basin, southwest Cameroon. *Heliyon*, 8(9), e10304.

2. Lim, D., Kim, J., Kim, W., et al. (2022). Characterization of geochemistry in hydrothermal sediments from the newly discovered Onnuri Vent Field in the middle region of the Central Indian Ridge. *Frontiers in Marine Science*, 9, 810949.

3. Alizadeh, Ak. A. (2005). Geology of Azerbaijan. Volume 4: Tectonics. *Baku: Nafta Press.*

4. Alizadeh, Ak. A. (2005). Geology of Azerbaijan. Volume 1. Stratigraphy, Part 2: Mesozoic and Cenozoic. *Baku: Nafta Press*.

5. Taylor, S. R., McLennan, S. M. (1985). The continental crust: its composition and evolution. *Blackwell Scientific*.

6. Boström, K. (1973). The origin and fate of ferromanganoan active ridge sediments. *Stockholm Contributions in Geology*, 27, 149–243.76.

7. Boström, K. (1983). Genesis of ferromanganese deposits—Diagnostic criteria for recent and old deposits /In: P. A. Rona (Ed.). Hydrothermal processes at seafloor spreading centers. *Boston, MA: Springer.*

8. Adachi, M., Yamamoto, K., Sugisaki, R. (1986). Hydrothermal cherts and associated siliceous rocks from northern Pacific: Their geological significance as indication of ocean ridge activity. *Sedimentary Geology*, 47(1–2), 125–148.

9. Qi, H., Hu, R., Su, W., et al. (2004). Continental hydrothermal sedimentary siliceous rock and genesis of superlarge germanium (Ge) deposit hosted in coal: A study from the Lincang Ge deposit, Yunnan, China. *Science in China Series D: Earth Sciences*, 47(11), 973–984.

10. Fedo, C. M., Nesbitt, H. W., Young, G. M. (1995). Unraveling the effects of potassium metasomatism in sedimentary rocks and paleosols, with implication for paleoweathering conditions and provenance. *Geology*, 23(10), 921–924.

11. Nesbitt, H. W., Young, G. M. (1989). Formation and diagenesis of weathering profiles. *The Journal of Geology*, 97(2), 129–147.

12. Panahi, A., Young, G. M., Rainbird, R. H. (2000). Behavior of major and trace elements (including REE) during Paleoproterozoic pedogenesis and diagenetic alteration of an Archean granite near Ville Marie, Quebec, Canada. *Geochimica et Cosmochimica Acta*, 64(13), 2199–2220.

13. Fathy, D., Abart, R., Wagreich, M., et al. (2023). Late Campanian climatic-continental weathering assessment and its influence on source rocks deposition in Southern Tethys, Egypt. *Minerals*, 13(2), 160.

14. Zhang, P., Meng, Q., Liu, Z., Hu, F. (2021). Mineralogy and geochemistry of the lower Cretaceous Jiufotang Formation, Beipiao Basin, NE China: Implications for weathering, provenance, and tectonic setting. *ACS Earth and Space Chemistry*, 5(6), 1288–1305.

15. Ivanova, V. V., Shchetnikov, A. A., Kiel, S. (2022). Sediment geochemistry of the section Tagay-1 at Olkhon Island (Lake Baikal, Eastern Siberia): A contribution to palaeoenvironmental interpretations. *Palaeobiodiversity and Palaeoenvironments*, 102(4), 921–941.

16. Roser, B. P., Korsch, R. J. (1988). Determination of tectonic setting of sandstone-mudstone suites using SiO_2 content and K_2O/Na_2O ratio. *The Journal of Geology*, 94(5), 635–650.

17. Verma, S. P., Armstrong-Altrin, J. S. (2013). New multidimensional diagrams for tectonic discrimination of siliciclastic sediments and their application to Precambrian basins. *Chemical Geology*, 355, 117–133.